SIMBIG: Galaxy Clustering beyond the Power Spectrum

ChangHoon Hahn [1] **Pablo Lemos** [2 3 4 5] **Liam Parker** [1] **Bruno Régaldo-Saint Blancard** [6] **Michael Eickenberg** [6]
Shirley Ho [5] **Jiamin Hou** [7 8] **Elena Massara** [9 10] **Chirag Modi** [5 6] **Azadeh Moradinezhad Dizgah** [11]
David Spergel [5 1]

Abstract

The study of the Universe revolves around understanding the fundamental parameters that describe the model of our Universe. These fundamental parameters are usually constrained by analyzing what we can observe from the sky such as galaxy distributions, the cosmic microwave background, etc. The paper uses the SIMBIG framework, which leverages machine learning techniques and simulation-based inference to improve the constraints on these fundamental parameters by analyzing galaxy clustering. When we apply SIMBIG to a fraction of the BOSS galaxy survey, we achieve significantly (1.2 and 2.7×) tighter constraints on cosmological parameters such as Ω_m and σ_8 compared to standard power spectrum analyses. Using only 10% of the BOSS volume, we obtain constraints on H_0 and S_8 that are competitive with those from other probes. Future work will extend SIMBIG to upcoming galaxy surveys for even stronger constraints.

[1]Department of Astrophysical Sciences, Princeton University, Princeton NJ 08544, USA [2]Department of Physics, Université de Montréal, Montréal, 1375 Avenue Thérèse-Lavoie-Roux, QC H2V 0B3, Canada [3]Mila - Quebec Artificial Intelligence Institute, Montréal, 6666 Rue Saint-Urbain, QC H2S 3H1, Canada [4]Ciela - Montreal Institute for Astrophysical Data Analysis and Machine Learning, Montréal, Canada [5]Center for Computational Astrophysics, Flatiron Institute, 162 5th Avenue, New York, NY 10010, USA [6]Center for Computational Mathematics, Flatiron Institute, 162 5th Avenue, New York, NY 10010, USA [7]Department of Astronomy, University of Florida, 211 Bryant Space Science Center, Gainesville, FL 32611, USA [8]Max-Planck-Institut für Extraterrestrische Physik, Postfach 1312, Giessenbachstrasse 1, 85748 Garching bei München, Germany [9]Waterloo Centre for Astrophysics, University of Waterloo, 200 University Ave W, Waterloo, ON N2L 3G1, Canada [10]Department of Physics and Astronomy, University of Waterloo, 200 University Ave W, Waterloo, ON N2L 3G1, Canada [11]Département de Physique Théorique, Université de Genève, 24 quai Ernest Ansermet, 1211 Genève 4, Switzerland. Correspondence to: ChangHoon Hahn <changhoon.hahn@princeton.edu>.

Proceedings of the 40^{th} International Conference on Machine Learning, Honolulu, Hawaii, USA. PMLR 202, 2023.

1. Introduction

The statistical clustering of galaxies provides key cosmological information that can be used to constrain the nature of our Universe. The next-generation galaxy surveys, such as DESI, PFS, Euclid, and Roman[1], will probe galaxies over unprecedented cosmic volumes. Combined with constraints from the cosmic microwave background (CMB) experiments, they will provide the most stringent tests of the cosmological model. The standard cosmological model (ΛCDM) has been remarkably successful at describing a wide range of cosmological observations including the accelerating expansion of the Universe (Perlmutter et al., 1999; Riess et al., 1998), the CMB (Page et al., 2003; Bennett et al., 2013; Collaboration et al., 2020; Aiola et al., 2020; Dutcher et al., 2021), and the large-scale structure (LSS; Bernardeau et al., 2002; Alam et al., 2017). The most statistically significant of the tensions in this model is the "Hubble tension", which refers to the disagreement between the late time measurements of the Hubble constant, H_0, with the inferred value from CMB assuming ΛCDM (see Abdalla et al., 2022; Shah et al., 2021, for recent reviews). In order to shed light on these model tensions, more observations and better analysis are needed.

Current analyses use the galaxy power spectrum as the primary measurement of galaxy clustering (*e.g.* Alam et al., 2017; Beutler et al., 2017; Ivanov et al., 2020; Chen et al., 2022; Kobayashi et al., 2022), focusing mainly on large, linear scales, where perturbation theory (PT; see Bernardeau et al., 2002; Desjacques et al., 2016, for a review) is valid. However, recent studies have established that there is significant additional information beyond these regimes on non-linear scales up to $k < 0.5\,h/\mathrm{Mpc}$ and in higher-order statistics (Hahn et al., 2020; Hahn & Villaescusa-Navarro, 2021; Massara et al., 2020; 2022; Wang et al., 2022; Hou et al., 2022; Eickenberg et al., 2022). Despite their promise, most higher-order statistics cannot be robustly analyzed using the standard PT approach, in part due to PT's inability to accurately model information on non-linear scales. Current analyses also struggle to account for observational systematics that significantly impact clustering measurements (*e.g.*

[1]desi.lbl.gov, pfs.ipmu.jp, sci.esa.int/web/euclid, and roman.gsfc.nasa.gov, respectively.

Ross et al., 2012; 2017).

Recently, Hahn et al. (2022) and Hahn et al. (2023) presented the Simulation-Based Inference of Galaxies (SIMBIG), a forward modeling framework for analyzing galaxy clustering. SIMBIG uses simulation-based inference (SBI; see Cranmer et al., 2020, for a review) to perform highly efficient cosmological parameter inference using neural density estimation from machine learning (*e.g.* Germain et al., 2015; Papamakarios et al., 2017). This enables SIMBIG to use high-fidelity simulations that model the full details of the observations. With this approach, Hahn et al. (2022) analyzed the power spectrum multipoles, $P_\ell(k)$, of 109,636 galaxies in the Sloan Digital Sky Survey (SDSS)-III Baryon Oscillation Spectroscopic Survey (BOSS; Eisenstein et al., 2011; Dawson et al., 2013) Southern Galactic Cap, and demonstrated that they can rigorously analyze the power spectrum down to smaller scales than ever before, $k_{\rm max} = 0.5\,h/{\rm Mpc}$.

In this work, we compare the cosmological constraints from three novel SIMBIG SBI analyses on the BOSS CMASS sample using various higher-order statistics to each other and to the constraints in previous literature.

2. SIMBIG

SIMBIG uses SBI to infer posteriors of the ΛCDM parameters with only summary statistics of a forward model simulation that can generate mock observations, *i.e.* the 3D galaxy spatial distribution, that are statistically indistinguishable from the BOSS CMASS catalogs. The specifics of the forward modelling pipeline are detailed in Appendix A. In this section, we briefly describe the SBI methodology, the statistics used, and the validation of the posteriors. More details about each of the statistics, how they are calculated, and the validation used will be presented in future work.

2.1. Simulation-Based Inference

From the forward modeled galaxy catalogs, we use the SIMBIG SBI framework to infer posterior distributions of cosmological parameters for given summary statistics of the observations (Hahn et al., 2022; 2023). The SBI framework uses Masked Autoregressive Flows (Greenberg et al., 2019; Tejero-Cantero et al., 2020) to approximate the posterior distribution of the cosmological parameters. Ultimately, we train a MAF that best approximates the posterior distribution $p(\boldsymbol{\theta}\,|\,\boldsymbol{x}) \approx q_{\boldsymbol{\phi}}(\boldsymbol{\theta}\,|\,\boldsymbol{x})$. In $q_{\boldsymbol{\phi}}(\boldsymbol{\theta}\,|\,\boldsymbol{x})$, $\boldsymbol{x}$ represents the summary statistic and $\boldsymbol{\theta}$ represents the 14 cosmological and HOD parameter. The prior of the posterior estimate is set by the parameter distribution of our training set. Since the N-body simulations used for our forward modeled catalogs are evaluated over a Latin-Hypercube configuration, we use uniform priors over the cosmological parameters, $\{\Omega_m, \Omega_b, h, n_s, \sigma_8\}$, with wide ranges that fully encompass the *Planck* priors. For the HOD parameters, we use the conservative priors centered around previous HOD analyses of the BOSS CMASS sample. For more details on the SBI approach, see Appendix B.

2.2. Statistics Beyond P_ℓ

With SIMBIG, we can derive cosmological constraints using any summary of the galaxy distribution that we can accurately forward model. In this work, we apply SIMBIG using three summaries: the bispectrum (B_0), wavelet scattering transform (WST) statistics, and a field-level summary with convolutional neural networks (CNN).

B(k_1, k_2, k_3): is the three-point correlation function in Fourier space. In this work, we use the monopole of the bispectrum: B_0. To measure B_0, we use the Fast Fourier Transform (FFT) based (Scoccimarro, 2015) redshift-space bispectrum estimator. For the observed galaxy sample, we also include angular systematic weights to account for stellar density and seeing conditions as well as redshift failure weights. We do not include weights for fiber collisions, since this effect is included in our forward model. We measure B_0 in triangle configurations defined by k_1, k_2, k_3 bins of width $\Delta k = 0.010472\,h/{\rm Mpc}$. For $k_{\rm max} = 0.5\,h/{\rm Mpc}$, B_0 has 10,052 total triangle configurations.

WST: defines a set of statistics well-suited to describing non-Gaussian physical fields (Bruna & Mallat, 2013; Mallat, 2016). WST consists of a cascade of convolutions with wavelets, pointwise non-linearities, and average pooling operators. It is motivated by the structure of CNNs while being completely parameter-free. These operations lead to a set of coefficients that quantify the amplitude of the input signal at a given oriented scale as well as couplings between oriented scales. We use WST that has been adapted to redshift-space data and capture information down to $k{\sim}0.5\,h/{\rm Mpc}$.

CNNs: can be thought of as flexible, hierarchical, non-linear functions that can be optimized to extract maximally relevant features from input images. In this work, we use a 3D CNN to perform a step of massive data compression from the density fields directly to the cosmological parameters (*e.g.* Jeffrey et al., 2021). The density fields are meshed to implicitly impose a scale cut of $k < k_{\rm max} = 0.57\,h/$Mpc. We train the CNN to compress the density fields by minimizing the mean-squared-error between the network-predicted cosmological parameters and the true parameters of the training simulations. Because of the significant epistemic uncertainty in the compression, we also perform Stochastic Weight Averaging (Maddox et al., 2019; Wilson & Izmailov, 2020), which leads to better generalization in SBI (Lemos et al., 2023b).

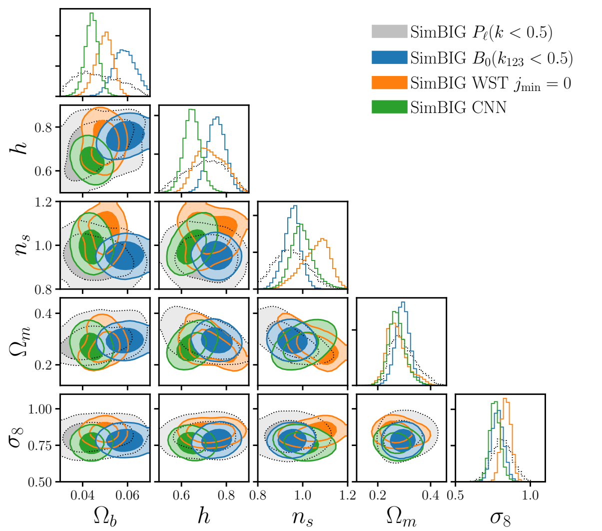

Figure 1. Marginalized 1D and 2D Posteriors of cosmological parameters inferred from B_0 (blue), WST (orange), and CNN (green) using SIMBIG. The contours mark the 68 and 95 percentiles of the posteriors. For comparison, we include the posterior from the SIMBIG P_ℓ analysis.

2.3. Validation

For each statistic, we validate the trained q_ϕ in two steps. First, we perform a coverage test, either using simulation-based calibration (Talts et al., 2020) or a "distance to random point" test (Lemos et al., 2023a), on a held out subset of the training data. With this test, we check whether q_ϕ is properly trained and accurately estimates the posterior throughout the prior range. Second, we assess the robustness of q_ϕ by applying it to the 2,000 "mock challenge" simulations (Hahn et al., 2023). These simulations include three different sets of test simulations evaluated at some fiducial cosmology, two of which ($\sim$ 1500 simulations) are generated using different forward models than the training set. We apply q_ϕ to the simulations and compare the resulting posteriors to the true parameter values of the simulations; if the q_ϕ posteriors of the two out-of-distribution suites are consistent with the true values, we conclude that q_ϕ is sufficiently robust.

3. Results

In Figure 1, we present the posteriors of the ΛCDM cosmological parameters for B_0 (blue), WST (orange), and CNN (green) SIMBIG analyses. For comparison, we include the posterior from the SIMBIG P_ℓ analysis (gray). In each of the contours we mark the 68 and 95 percentiles of the posteriors. The posteriors are derived from galaxy clustering alone and do not rely on any BBN or CMB priors. Overall, the SIMBIG posteriors are statistically consistent.

For WST, we find that the constraints for Ω_b and σ_8 are 1.83 and 2.84$\times$ tighter than the results of Ivanov et al. (2020)

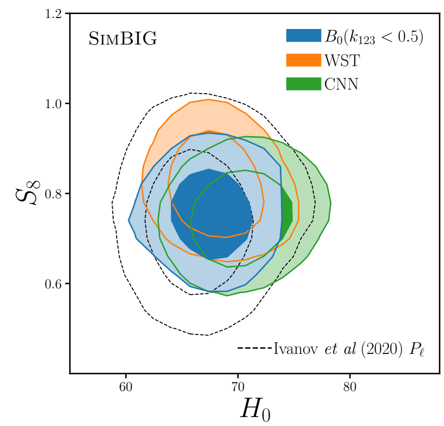

Figure 2. S_8 and H_0 posteriors for the SIMBIG B_0 (blue), WST (orange), and CNN (green) analyses. We include the posterior from the I20 P_ℓ analyses of CMASS-SGC, for comparison (black dashed). All of the posteriors include a ω_b prior from BBN studies. With higher-order statistics, our S_8 and H_0 constraints are 1.92 and 1.51$\times$ tighter than the standard P_ℓ constraints.

(hereafter I20) P_ℓ. Meanwhile, WST does not improve Ω_m, h, and n_s constraints. The improvement of WST over P_ℓ is more modest than in the forecasts (Eickenberg et al., 2022). This is because we discard a significant amount of cosmological information in our analysis to ensure robustness. For B_0, our constraints are 1.40, 1.41, and 1.69$\times$ tighter than the I20 analysis for Ω_b, h, and n_s, respectively. Meanwhile, for Ω_m and σ_8, B_0 is , 1.18 and 2.35$\times$ tighter than I20. For CNN, the constraints are 2.40, 1.52, and 1.30$\times$ tighter than I20 constraints for Ω_b, h, n_s. For Ω_m and σ_8, our constraints are 1.03 and 2.65$\times$ more precise. In principle, the CNN is capable of extracting even more cosmological information from the galaxy field; however, similar to the WST analysis, we restrict this to ensure robustness.

Overall, the SIMBIG higher-order clustering analyses produce significantly tighter cosmological constraints than the I20 P_ℓ analyses. Together, B_0, WST, and CNN improve Ω_m, Ω_b, h, n_s, and σ_8 by factors of 1.18, 2.40, 1.52, 1.69, and 2.65 respectively. This is in spite of the fact that we severely limit our WST and CNN analyses for robustness. Nevertheless, our results firmly demonstrate that there is significant additional non-Gaussian cosmological information. More importantly, SIMBIG analyses are able to robustly extract this information from observational data.

3.1. Cosmic Tensions

Our tighter constraints on cosmological parameters can also inform the potential "cosmic tensions" — *i.e.* the discrepancy between early and late universe measurements of $S_8 = \sigma_8\sqrt{\Omega_m/0.3}$ and H_0 (Abdalla et al., 2022). In Figure 2, we present the S_8 and H_0 posteriors from the SIMBIG analyses of B_0 (blue), WST (orange), and CNN (green). For comparison, we also plot the posterior for the I20 P_ℓ analysis of CMASS-SGC (black dashed). For these posteriors, we impose a prior on ω_b from BBN studies (Aver et al., 2015; Cooke et al., 2018; Schöneberg et al., 2019).

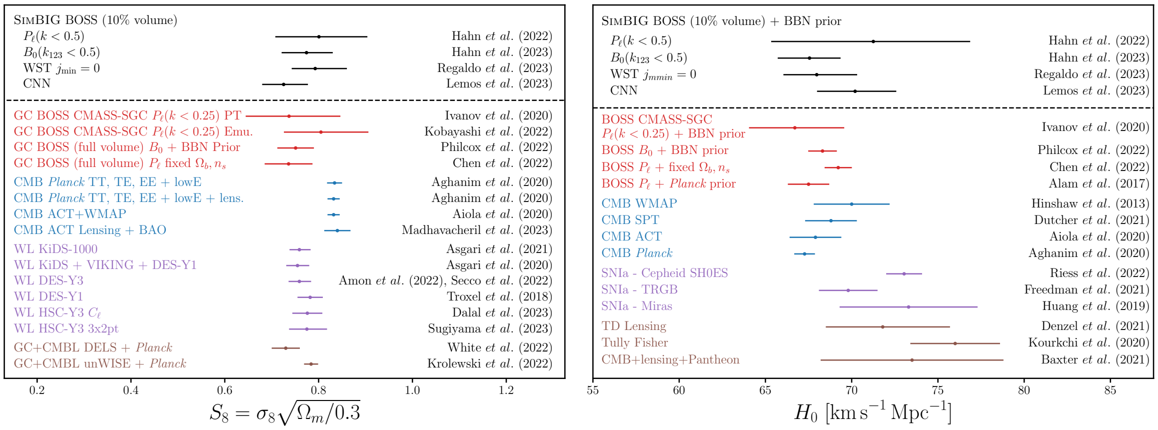

Figure 3. Comparison of the SIMBIG constraints to constraints in the literature from different cosmological probes for S_8 (top) and H_0 (bottom). For the SIMBIG H_0 constraint, we include a ω_b prior from BBN. The constraints from the literature are compiled from (Abdalla et al., 2022). Our S_8 constraints are consistent with both CMB and weak lensing constraints. Meanwhile our H_0 constraints are consistent with CMB and in tension with supernovae constraints. Despite only using 10% of the BOSS volume, we derive constraints that are competitive with other cosmological probes.

This prior significantly tightens our H_0 posteriors but does not impact our S_8 constraints. Our S_8 and H_0 constraints from B_0, WST, and CNN are highly consistent with each other. Compared to I20, we improve S_8 by 1.92, 1.52, and 1.83×. They improve H_0 by 1.51, 1.29, and 1.20×.

Next we compare our S_8 and H_0 posteriors to constraints in the literature from galaxy clustering and other cosmological probes (Figure 3). The constraints from the literature are selected from (Abdalla et al., 2022). In the top panel, we compare the SIMBIG S_8 constraints (black) to constraints from galaxy clustering (red), CMB (blue), weak lensing (purple), and multi-probe (brown). Despite only analyzing 10% of the total BOSS volume, the SIMBIG higher-order statistics analyses produce S_8 constraints with precision comparable to P_ℓ analyses of the full BOSS volume. Furthermore, the S_8 constraints from the SIMBIG P_ℓ, B_0, and WST analyses are statistically consistent with both CMB and weak lensing. They lie in between the two probes and slightly above the other BOSS galaxy clustering constraints.

Next, in the bottom panel of Figure 3, we compare the SIMBIG H_0 posteriors to constraints from wide variety of cosmological probes: galaxy clustering (red), CMB (blue), supernovae-Ia (SNIa; purple), and others (brown) compiled from (Abdalla et al., 2022). The SIMBIG constraints are significantly lower than the SNIa constraints and in good agreement with CMB and other galaxy clustering constraints.

3.2. Upcoming Surveys and Future Steps

Despite only using 10% of the BOSS volume, we derive S_8 and H_0 constraints that are competitive with other cosmological probes and clustering analyses of the full BOSS volume. This is driven by the higher-order and non-linear cosmological information we are able to robustly extract with the SIMBIG approach. In short, our forward modeling approach improves S_8 and H_0 constraints by ~2.0 and 1.5× over the standard PT P_ℓ analysis. This improvement is equivalent to applying the PT P_ℓ analysis to a galaxy sample that spans *more than double* the cosmic volume.

Yet, the improvement does not include *all* of the cosmological information that can be extracted using higher-order clustering statistics. For the WST and CNN, our constraints are severely limited by robustness. We require the SIMBIG WST and CNN analyses to derive unbiased cosmological constraints for a suite of test simulations constructed with different forward models (Section 2.3). These procedures discard a substantial amount of cosmological information that we could otherwise recover, *if* we had a sufficiently flexible forward model that could simultaneously describe the training and test simulations. This would, however, require developing a more flexible halo finder and HOD model. We will explore this in future work.

In future work, we will extend SIMBIG to the next generation spectroscopic galaxy surveys: *e.g.* DESI, PFS, and *Euclid*. These surveys will probe enormous cosmic volumes with tens of millions of galaxies in epochs without precise H_0 or S_8 constraints from other cosmological probes. We highlight this in Figure 4, where we present the expected 1σ values of H_0 (top) and S_8 (bottom) constraints from applying SIMBIG to DESI, PFS, and *Euclid* (black). The forecasts are derived by scaling the SIMBIG constraints by the volume of the suryve. For H_0, upcoming surveys will help bridge the gap between the late-time measurements from SNe-Ia (SH0ES; red) and early-time measurements from the CMB (*Planck*; blue). H_0 constraints from other probes, *e.g.* time delay lensing, have significantly larger uncertainties that lie outside the range of the figure. Similarly, for S_8, DESI, PFS, and *Euclid* will bridge the gap between S_8 constraints from weak lensing surveys that probe LSS at low redshifts and from CMB lensing and CMB at high redshifts. The shaded regions represent the lensing efficiency kernel for weak lensing experiments ($0.1 < z < 0.7$; Amon et al., 2022) and the mass-map weights for CMB lensing ($0.5 < z < 5.0$; Madhavacheril et al., 2023).

Figure 4 demonstrates that by more fully extracting the cosmological information of upcoming galaxy surveys, SIMBIG can produce leading constraints on both S_8 and H_0. With their precision levels and the extensive redshift range of DESI and PFS, future SIMBIGanalyses will provide critical input into the cosmic tensions and potentially reveal new physics beyond the standard ΛCDM model.

In future work, we will address the computational challenges of extending SIMBIG to larger volumes. We will explore the use of more efficient approximate N-body schemes (Feng et al., 2016; Modi et al., 2021) and recent GPU implementations that accelerate them even further (Li et al., 2022). We will also investigate the use of ML methods for enhancing their accuracy (Dai et al., 2020; Schaurecker et al., 2021; Jamieson et al., 2022).

References

Abdalla, E., Abellán, G. F., Aboubrahim, A., Agnello, A., Akarsu, Ö., Akrami, Y., Alestas, G., Aloni, D., Amendola, L., Anchordoqui, L. A., Anderson, R. I., Arendse, N., Asgari, M., Ballardini, M., Barger, V., Basilakos, S., Batista, R. C., Battistelli, E. S., Battye, R., Benetti, M., Benisty, D., Berlin, A., de Bernardis, P., Berti, E., Bidenko, B., Birrer, S., Blakeslee, J. P., Boddy, K. K., Bom, C. R., Bonilla, A., Borghi, N., Bouchet, F. R., Braglia, M., Buchert, T., Buckley-Geer, E., Calabrese, E., Caldwell, R. R., Camarena, D., Capozziello, S., Casertano, S., Chen, G. C. F., Chluba, J., Chen, A., Chen, H.-Y., Chudaykin, A., Cicoli, M., Copi, C. J., Courbin, F., Cyr-Racine, F.-Y., Czerny, B., Dainotti, M., D'Amico, G., Davis, A.-C., de Cruz Pérez, J., de Haro, J., Delabrouille, J., Denton, P. B., Dhawan, S., Dienes, K. R., Di Valentino, E., Du, P., Eckert, D., Escamilla-Rivera, C., Ferté, A., Finelli, F., Fosalba, P., Freedman, W. L., Frusciante, N., Gaztañaga, E., Giarè, W., Giusarma, E., Gómez-Valent, A., Handley, W., Harrison, I., Hart, L., Hazra, D. K., Heavens, A., Heinesen, A., Hildebrandt, H., Hill, J. C., Hogg, N. B., Holz, D. E., Hooper, D. C., Hosseininejad, N., Huterer, D., Ishak, M., Ivanov, M. M., Jaffe, A. H., Jang, I. S., Jedamzik, K., Jimenez, R., Joseph, M., Joudaki, S., Kamionkowski, M., Karwal, T., Kazantzidis, L., Keeley, R. E., Klasen, M., Komatsu, E., Koopmans, L. V. E., Kumar, S., Lamagna, L., Lazkoz, R., Lee, C.-C., Lesgourgues, J., Levi Said, J., Lewis, T. R., L'Huillier, B., Lucca, M., Maartens, R., Macri, L. M., Marfatia, D., Marra, V., Martins, C. J. A. P., Masi, S., Matarrese, S., Mazumdar, A., Melchiorri, A., Mena, O., Mersini-Houghton, L., Mertens, J., Milaković, D., Minami, Y., Miranda, V., Moreno-Pulido, C., Moresco, M., Mota, D. F., Mottola, E., Mozzon, S., Muir, J., Mukherjee, A., Mukherjee, S., Naselsky, P., Nath, P., Nesseris, S., Niedermann, F., Notari, A., Nunes, R. C., Ó Colgáin, E., Owens, K. A., Özülker, E., Pace, F., Paliathanasis, A., Palmese, A., Pan, S., Paoletti, D., Perez Bergliaffa, S. E., Perivolaropoulos, L., Pesce, D. W., Pettorino, V., Philcox, O. H. E., Pogosian, L., Poulin, V., Poulot, G., Raveri, M., Reid, M. J., Renzi, F., Riess, A. G., Sabla, V. I., Salucci, P., Salzano, V., Saridakis, E. N., Sathyaprakash, B. S., Schmaltz, M., Schöneberg, N., Scolnic, D., Sen, A. A., Sehgal, N., Shafieloo, A., Sheikh-Jabbari, M. M., Silk, J., Silvestri, A., Skara, F., Sloth, M. S., Soares-Santos, M., Solà Peracaula, J., Songsheng, Y.-Y., Soriano, J. F., Staicova, D., Starkman, G. D., Szapudi, I., Teixeira, E. M., Thomas, B., Treu, T., Trott, E., van de Bruck, C., Vazquez, J. A., Verde, L., Visinelli, L., Wang, D., Wang, J.-M., Wang, S.-J., Watkins, R., Watson, S., Webb, J. K., Weiner, N., Weltman, A., Witte, S. J., Wojtak, R., Yadav, A. K., Yang, W., Zhao, G.-B., and Zumalacárregui, M. Cosmology intertwined: A review of the particle physics, astrophysics, and cosmology associated with the cosmological tensions and anomalies. *Journal of High Energy Astrophysics*, 34:49–211, June 2022. doi: 10.1016/j.jheap.2022.04.002.

Aiola, S., Calabrese, E., Maurin, L., Naess, S., Schmitt, B. L., Abitbol, M. H., Addison, G. E., Ade, P. A., Alonso, D., Amiri, M., et al. The atacama cosmology telescope: Dr4 maps and cosmological parameters. *Journal of Cosmology and Astroparticle Physics*, 2020(12):047, 2020.

Alam, S., Ata, M., Bailey, S., Beutler, F., Bizyaev, D., Blazek, J. A., Bolton, A. S., Brownstein, J. R., Burden, A., Chuang, C.-H., Comparat, J., Cuesta, A. J., Dawson, K. S., Eisenstein, D. J., Escoffier, S., Gil-Marín, H., Grieb, J. N., Hand, N., Ho, S., Kinemuchi, K., Kirkby, D., Kitaura, F., Malanushenko, E., Malanushenko, V., Maraston, C., McBride, C. K., Nichol, R. C., Olmstead, M. D., Oravetz, D., Padmanabhan, N., Palanque-Delabrouille, N., Pan, K., Pellejero-Ibanez, M., Percival, W. J., Petitjean, P., Prada, F., Price-Whelan, A. M., Reid, B. A., Rodríguez-Torres, S. A., Roe, N. A., Ross, A. J., Ross, N. P., Rossi, G., Rubiño-Martín, J. A., Saito, S., Salazar-Albornoz, S., Samushia, L., Sánchez, A. G., Satpathy, S., Schlegel, D. J., Schneider, D. P., Scóccola, C. G., Seo, H.-J., Sheldon, E. S., Simmons, A., Slosar, A., Strauss, M. A., Swanson, M. E. C., Thomas, D., Tinker, J. L., Tojeiro, R., Magaña, M. V., Vazquez, J. A., Verde, L., Wake, D. A., Wang, Y., Weinberg, D. H., White, M., Wood-Vasey, W. M., Yèche, C., Zehavi, I., Zhai, Z., and Zhao, G.-B. The clustering of galaxies in the completed SDSS-III Baryon Oscillation Spectroscopic Survey: cosmological analysis of the DR12 galaxy sample. , 470(3): 2617–2652, September 2017. doi: 10.1093/mnras/stx721.

Amon, A., Gruen, D., Troxel, M. A., MacCrann, N., Dodelson, S., Choi, A., Doux, C., Secco, L. F., Samuroff, S., Krause, E., Cordero, J., Myles, J., DeRose, J., Wechsler, R. H., Gatti, M., Navarro-Alsina, A., Bernstein, G. M., Jain, B., Blazek, J., Alarcon, A., Ferté, A., Lemos, P., Raveri, M., Campos, A., Prat, J., Sánchez, C., Jarvis, M., Alves, O., Andrade-Oliveira, F., Baxter, E., Bechtol, K., Becker, M. R., Bridle, S. L., Camacho, H., Carnero Rosell, A., Carrasco Kind, M., Cawthon, R., Chang, C., Chen, R., Chintalapati, P., Crocce, M., Davis, C., Diehl, H. T., Drlica-Wagner, A., Eckert, K., Eifler, T. F., Elvin-Poole, J., Everett, S., Fang, X., Fosalba, P., Friedrich, O., Gaztanaga, E., Giannini, G., Gruendl, R. A., Harrison, I., Hartley, W. G., Herner, K., Huang, H., Huff, E. M., Huterer, D., Kuropatkin, N., Leget, P., Liddle, A. R., McCullough, J., Muir, J., Pandey, S., Park, Y., Porredon, A., Refregier, A., Rollins, R. P., Roodman, A., Rosenfeld, R., Ross, A. J., Rykoff, E. S., Sanchez, J., Sevilla-Noarbe, I., Sheldon, E., Shin, T., Troja, A., Tutusaus, I., Tutusaus, I., Varga, T. N., Weaverdyck, N., Yanny, B., Yin, B., Zhang, Y., Zuntz, J., Aguena, M., Allam, S., Annis, J., Bacon, D., Bertin, E., Bhargava, S., Brooks, D., Buckley-Geer, E., Burke, D. L., Carretero, J., Costanzi, M., da Costa, L. N., Pereira, M. E. S., De Vicente, J., Desai, S., Dietrich, J. P., Doel, P., Ferrero, I., Flaugher, B., Frieman, J., García-Bellido, J., Gaztanaga, E., Gerdes, D. W., Giannantonio, T., Gschwend, J., Gutierrez, G., Hinton, S. R., Hollowood, D. L., Honscheid, K., Hoyle, B., James, D. J., Kron, R., Kuehn, K., Lahav, O., Lima, M., Lin, H., Maia, M. A. G., Marshall, J. L., Martini, P., Melchior, P., Menanteau, F., Miquel, R., Mohr, J. J., Morgan, R., Ogando, R. L. C., Palmese, A., Paz-Chinchón, F., Petravick, D., Pieres, A., Romer, A. K., Sanchez, E., Scarpine, V., Schubnell, M., Serrano, S., Smith, M., Soares-Santos, M., Tarle, G., Thomas, D., To, C., Weller, J., and DES Collaboration. Dark Energy Survey Year 3 results: Cosmology from cosmic shear and robustness to data calibration. , 105(2):023514, January 2022. doi: 10.1103/PhysRevD.105.023514.

Aver, E., Olive, K. A., and Skillman, E. D. The effects of He I λ10830 on helium abundance determinations. , 2015 (7):011–011, July 2015. doi: 10.1088/1475-7516/2015/07/011.

Behroozi, P. S., Wechsler, R. H., and Wu, H.-Y. The ROCKSTAR Phase-space Temporal Halo Finder and the Velocity Offsets of Cluster Cores. *The Astrophysical Journal*, 762:109, January 2013. ISSN 0004-637X. doi: 10.1088/0004-637X/762/2/109.

Bennett, C. L., Larson, D., Weiland, J. L., Jarosik, N., Hinshaw, G., Odegard, N., Smith, K., Hill, R., Gold, B., Halpern, M., et al. Nine-year wilkinson microwave anisotropy probe (wmap) observations: final maps and results. *The Astrophysical Journal Supplement Series*, 208(2):20, 2013.

Berlind, A. A. and Weinberg, D. H. The Halo Occupation Distribution: Toward an Empirical Determination of the Relation between Galaxies and Mass. , 575(2):587–616, August 2002. doi: 10.1086/341469.

Bernardeau, F., Colombi, S., Gaztanaga, E., and Scoccimarro, R. Large-Scale Structure of the Universe and Cosmological Perturbation Theory. *Physics Reports*, 367 (1-3):1–248, September 2002. ISSN 03701573. doi: 10.1016/S0370-1573(02)00135-7.

Beutler, F., Seo, H.-J., Saito, S., Chuang, C.-H., Cuesta, A. J., Eisenstein, D. J., Gil-Marín, H., Grieb, J. N., Hand, N., Kitaura, F.-S., Modi, C., Nichol, R. C., Olmstead, M. D., Percival, W. J., Prada, F., Sánchez, A. G., Rodriguez-Torres, S., Ross, A. J., Ross, N. P., Schneider, D. P., Tinker, J., Tojeiro, R., and Vargas-Magaña, M. The clustering of galaxies in the completed SDSS-III Baryon Oscillation Spectroscopic Survey: Anisotropic galaxy clustering in Fourier space. *Monthly Notices of the Royal Astronomical Society*, 466:2242–2260, April 2017. ISSN 0035-8711. doi: 10.1093/mnras/stw3298.

Bruna, J. and Mallat, S. Invariant scattering convolution networks. *IEEE Transactions on Pattern Analysis and Machine Intelligence*, 35(8):1872–1886, 2013. doi: 10.1109/TPAMI.2012.230.

Chen, S.-F., Vlah, Z., and White, M. A new analysis of galaxy 2-point functions in the BOSS survey, including full-shape information and post-reconstruction BAO. , 2022(2):008, February 2022. doi: 10.1088/1475-7516/2022/02/008.

Collaboration, P., Aghanim, N., Akrami, Y., Ashdown, M., Aumont, J., Baccigalupi, C., Ballardini, M., Banday, A., Barreiro, R., Bartolo, N., et al. Planck 2018 results. vi. cosmological parameters. 2020.

Cooke, R. J., Pettini, M., and Steidel, C. C. One Percent Determination of the Primordial Deuterium Abundance. , 855(2):102, March 2018. doi: 10.3847/1538-4357/aaab53.

Cranmer, K., Brehmer, J., and Louppe, G. The frontier of simulation-based inference. *Proceedings of the National Academy of Sciences*, 117(48):30055–30062, 2020. ISSN 0027-8424. doi: 10.1073/pnas.1912789117.

Dai, B., Feng, Y., Seljak, U., and Singh, S. High mass and halo resolution from fast low resolution simulations. *Journal of Cosmology and Astroparticle Physics*, 2020:002, April 2020. ISSN 1475-7516. doi: 10.1088/1475-7516/2020/04/002.

Dawson, K. S., Schlegel, D. J., Ahn, C. P., Anderson, S. F., Aubourg, É., Bailey, S., Barkhouser, R. H., Bautista, J. E., Beifiori, A., Berlind, A. A., Bhardwaj, V., Bizyaev, D., Blake, C. H., Blanton, M. R., Blomqvist, M., Bolton, A. S., Borde, A., Bovy, J., Brandt, W. N., Brewington, H., Brinkmann, J., Brown, P. J., Brownstein, J. R., Bundy, K., Busca, N. G., Carithers, W., Carnero, A. R., Carr, M. A., Chen, Y., Comparat, J., Connolly, N., Cope, F., Croft, R. A. C., Cuesta, A. J., da Costa, L. N., Davenport, J. R. A., Delubac, T., de Putter, R., Dhital, S., Ealet, A., Ebelke, G. L., Eisenstein, D. J., Escoffier, S., Fan, X., Filiz Ak, N., Finley, H., Font-Ribera, A., Génova-Santos, R., Gunn, J. E., Guo, H., Haggard, D., Hall, P. B., Hamilton, J.-C., Harris, B., Harris, D. W., Ho, S., Hogg, D. W., Holder, D., Honscheid, K., Huehnerhoff, J., Jordan, B., Jordan, W. P., Kauffmann, G., Kazin, E. A., Kirkby, D., Klaene, M. A., Kneib, J.-P., Le Goff, J.-M., Lee, K.-G., Long, D. C., Loomis, C. P., Lundgren, B., Lupton, R. H., Maia, M. A. G., Makler, M., Malanushenko, E., Malanushenko, V., Mandelbaum, R., Manera, M., Maraston, C., Margala, D., Masters, K. L., McBride, C. K., McDonald, P., McGreer, I. D., McMahon, R. G., Mena, O., Miralda-Escudé, J., Montero-Dorta, A. D., Montesano, F., Muna, D., Myers, A. D., Naugle, T., Nichol, R. C., Noterdaeme, P., Nuza, S. E., Olmstead, M. D., Oravetz, A., Oravetz, D. J., Owen, R., Padmanabhan, N., Palanque-Delabrouille, N., Pan, K., Parejko, J. K., Pâris, I., Percival, W. J., Pérez-Fournon, I., Pérez-Ràfols, I., Petitjean, P., Pfaffenberger, R., Pforr, J., Pieri, M. M., Prada, F., Price-Whelan, A. M., Raddick, M. J., Rebolo, R., Rich, J., Richards, G. T., Rockosi, C. M., Roe, N. A., Ross, A. J., Ross, N. P., Rossi, G., Rubiño-Martin, J. A., Samushia, L., Sánchez, A. G., Sayres, C., Schmidt, S. J., Schneider, D. P., Scóccola, C. G., Seo, H.-J., Shelden, A., Sheldon, E., Shen, Y., Shu, Y., Slosar, A., Smee, S. A., Snedden, S. A., Stauffer, F., Steele, O., Strauss, M. A., Streblyanska, A., Suzuki, N., Swanson, M. E. C., Tal, T., Tanaka, M., Thomas, D., Tinker, J. L., Tojeiro, R., Tremonti, C. A., Vargas Magaña, M., Verde, L., Viel, M., Wake, D. A., Watson, M., Weaver, B. A., Weinberg, D. H., Weiner, B. J., West, A. A., White, M., Wood-Vasey, W. M., Yeche, C., Zehavi, I., Zhao, G.-B., and Zheng, Z. The Baryon Oscillation Spectroscopic Survey of SDSS-III. *The Astronomical Journal*, 145:10, January 2013. ISSN 0004-6256. doi: 10.1088/0004-6256/145/1/10.

Desjacques, V., Jeong, D., and Schmidt, F. Large-Scale Galaxy Bias. *arXiv:1611.09787 [astro-ph, physics:gr-qc, physics:hep-ph]*, November 2016.

Dutcher, D., Balkenhol, L., Ade, P., Ahmed, Z., Anderes, E., Anderson, A., Archipley, M., Avva, J., Aylor, K., Barry, P., et al. Measurements of the e-mode polarization and temperature-e-mode correlation of the cmb from spt-3g 2018 data. *Physical Review D*, 104(2):022003, 2021.

Eickenberg, M., Allys, E., Moradinezhad Dizgah, A., Lemos, P., Massara, E., Abidi, M., Hahn, C., Hassan, S., Regaldo-Saint Blancard, B., Ho, S., Mallat, S., Andén, J., and Villaescusa-Navarro, F. Wavelet Moments for Cosmological Parameter Estimation, April 2022.

Eisenstein, D. J., Weinberg, D. H., Agol, E., Aihara, H., Allende Prieto, C., Anderson, S. F., Arns, J. A., Aubourg, É., Bailey, S., Balbinot, E., Barkhouser, R., Beers, T. C., Berlind, A. A., Bickerton, S. J., Bizyaev, D., Blanton, M. R., Bochanski, J. J., Bolton, A. S., Bosman, C. T., Bovy, J., Brandt, W. N., Breslauer, B., Brewington, H. J., Brinkmann, J., Brown, P. J., Brownstein, J. R., Burger, D., Busca, N. G., Campbell, H., Cargile, P. A., Carithers, W. C., Carlberg, J. K., Carr, M. A., Chang, L., Chen, Y., Chiappini, C., Comparat, J., Connolly, N., Cortes, M., Croft, R. A. C., Cunha, K., da Costa, L. N., Davenport, J. R. A., Dawson, K., De Lee, N., Porto de Mello, G. F., de Simoni, F., Dean, J., Dhital, S., Ealet, A., Ebelke, G. L., Edmondson, E. M., Eiting, J. M., Escoffier, S., Esposito, M., Evans, M. L., Fan, X., Femenía Castellá, B., Dutra Ferreira, L., Fitzgerald, G., Fleming, S. W., Font-Ribera, A., Ford, E. B., Frinchaboy, P. M., García Pérez, A. E., Gaudi, B. S., Ge, J., Ghezzi, L., Gillespie, B. A., Gilmore, G., Girardi, L., Gott, J. R., Gould, A., Grebel, E. K., Gunn, J. E., Hamilton, J.-C., Harding, P., Harris, D. W., Hawley, S. L., Hearty, F. R., Hennawi, J. F., González Hernández, J. I., Ho, S., Hogg, D. W., Holtzman, J. A., Honscheid, K., Inada, N., Ivans, I. I., Jiang, L., Jiang, P., Johnson, J. A., Jordan, C., Jordan, W. P., Kauffmann, G., Kazin, E., Kirkby, D., Klaene, M. A., Knapp, G. R., Kneib, J.-P., Kochanek, C. S., Koesterke, L., Kollmeier, J. A., Kron, R. G., Lampeitl, H., Lang, D., Lawler, J. E., Le Goff, J.-M., Lee, B. L., Lee, Y. S., Leisenring, J. M., Lin, Y.-T., Liu, J., Long, D. C., Loomis, C. P., Lucatello, S., Lundgren, B., Lupton, R. H., Ma, B., Ma, Z., MacDonald, N., Mack, C., Mahadevan, S., Maia, M. A. G., Majewski, S. R., Makler, M., Malanushenko, E., Malanushenko, V., Mandelbaum, R., Maraston, C., Margala, D., Maseman, P., Masters, K. L., McBride, C. K., McDonald, P., McGreer, I. D., McMahon, R. G., Mena Requejo, O., Ménard, B., Miralda-Escudé, J., Morrison, H. L., Mullally, F., Muna, D., Murayama, H., Myers, A. D., Naugle, T., Neto, A. F., Nguyen, D. C., Nichol, R. C., Nidever, D. L., O'Connell, R. W., Ogando, R. L. C., Olmstead, M. D., Oravetz, D. J., Padmanabhan, N., Paegert, M., Palanque-Delabrouille, N., Pan, K., Pandey, P., Parejko, J. K., Pâris, I., Pellegrini, P., Pepper, J., Percival, W. J., Petitjean, P., Pfaffenberger, R., Pforr, J., Phleps, S., Pichon, C., Pieri, M. M., Prada, F., Price-Whelan, A. M., Raddick, M. J., Ramos, B. H. F., Reid, I. N., Reyle, C., Rich, J., Richards, G. T., Rieke, G. H., Rieke, M. J., Rix, H.-W., Robin, A. C., Rocha-Pinto, H. J., Rockosi, C. M., Roe, N. A., Rollinde, E., Ross, A. J., Ross, N. P., Rossetto, B., Sánchez, A. G., Santiago, B., Sayres, C., Schiavon, R., Schlegel, D. J., Schlesinger, K. J., Schmidt, S. J., Schneider, D. P., Sellgren, K., Shelden, A., Sheldon, E., Shetrone, M., Shu, Y., Silverman, J. D., Simmerer, J., Simmons, A. E., Sivarani, T., Skrutskie, M. F., Slosar, A., Smee, S., Smith, V. V., Snedden, S. A., Stassun, K. G., Steele, O., Steinmetz, M., Stockett, M. H., Stollberg, T., Strauss, M. A., Szalay, A. S., Tanaka, M., Thakar, A. R., Thomas, D., Tinker, J. L., Tofflemire, B. M., Tojeiro, R., Tremonti, C. A., Vargas Magaña, M., Verde, L., Vogt, N. P., Wake, D. A., Wan, X., Wang, J., Weaver, B. A., White, M., White, S. D. M., Wilson, J. C., Wisniewski, J. P., Wood-Vasey, W. M., Yanny, B., Yasuda, N., Yèche, C., York, D. G., Young, E., Zasowski, G., Zehavi, I., and Zhao, B. SDSS-III: Massive Spectroscopic Surveys of the Distant Universe, the Milky Way, and Extra-Solar Planetary Systems. *The Astronomical Journal*, 142:72, September 2011. ISSN 0004-6256. doi: 10.1088/0004-6256/142/3/72.

Feng, Y., Chu, M.-Y., Seljak, U., and McDonald, P. FASTPM: A new scheme for fast simulations of dark matter and haloes. *Monthly Notices of the Royal Astronomical Society*, 463:2273–2286, December 2016. ISSN 0035-8711. doi: 10.1093/mnras/stw2123.

Germain, M., Gregor, K., Murray, I., and Larochelle, H. MADE: Masked Autoencoder for Distribution Estimation. *Proceedings of the 32nd International Conference on Machine Learning*, 37:881–889, June 2015.

Greenberg, D. S., Nonnenmacher, M., and Macke, J. H. Automatic Posterior Transformation for Likelihood-Free Inference, May 2019.

Hahn, C. and Villaescusa-Navarro, F. Constraining Mν with the bispectrum. Part II. The information content of the galaxy bispectrum monopole. *Journal of Cosmology and Astroparticle Physics*, 2021:029, April 2021. ISSN 1475-7516. doi: 10.1088/1475-7516/2021/04/029.

Hahn, C., Villaescusa-Navarro, F., Castorina, E., and Scoccimarro, R. Constraining Mν with the bispectrum. Part I. Breaking parameter degeneracies. *Journal of Cosmology and Astroparticle Physics*, 03:040, March 2020. ISSN 1475-7516. doi: 10.1088/1475-7516/2020/03/040.

Hahn, C., Eickenberg, M., Ho, S., Hou, J., Lemos, P., Massara, E., Modi Chirag, Moradinezhad Dizgah, A., Régaldo-Saint Blancard, B., and Abidi, M. M. SimBIG: A Forward Modeling Approach To Analyzing Galaxy Clustering. 2022.

Hahn, C., Eickenberg, M., Ho, S., Hou, J., Lemos, P., Massara, E., Modi, C., Moradinezhad Dizgah, A., Régaldo-Saint Blancard, B., and Abidi, M. M. SIMBIG: mock challenge for a forward modeling approach to galaxy clustering. , 2023(4):010, April 2023. doi: 10.1088/1475-7516/2023/04/010.

Hearin, A. P., Zentner, A. R., van den Bosch, F. C., Campbell, D., and Tollerud, E. Introducing decorated HODs: Modelling assembly bias in the galaxy-halo connection. *Monthly Notices of the Royal Astronomical Society*, 460:2552–2570, August 2016. ISSN 0035-8711. doi: 10.1093/mnras/stw840.

Hou, J., Moradinezhad Dizgah, A., Hahn, C., and Massara, E. Cosmological Information in Skew Spectra of Biased Tracers in Redshift Space. *arXiv e-prints*, art. arXiv:2210.12743, October 2022.

Ivanov, M. M., Simonović, M., and Zaldarriaga, M. Cosmological parameters from the BOSS galaxy power spectrum. *Journal of Cosmology and Astroparticle Physics*, 2020:042, May 2020. ISSN 1475-7516. doi: 10.1088/1475-7516/2020/05/042.

Jamieson, D., Li, Y., Alves de Oliveira, R., Villaescusa-Navarro, F., Ho, S., and Spergel, D. N. Field Level Neural Network Emulator for Cosmological N-body Simulations, June 2022.

Jeffrey, N., Alsing, J., and Lanusse, F. Likelihood-free inference with neural compression of DES SV weak lensing map statistics. *Monthly Notices of the Royal Astronomical Society*, 501:954–969, February 2021. ISSN 0035-8711. doi: 10.1093/mnras/staa3594.

Kingma, D. P. and Ba, J. Adam: A Method for Stochastic Optimization. *arXiv:1412.6980 [cs]*, January 2017.

Knebe, A., Knollmann, S. R., Muldrew, S. I., Pearce, F. R., Aragon-Calvo, M. A., Ascasibar, Y., Behroozi, P. S., Ceverino, D., Colombi, S., Diemand, J., Dolag, K., Falck, B. L., Fasel, P., Gardner, J., Gottlöber, S., Hsu, C.-H., Iannuzzi, F., Klypin, A., Lukić, Z., Maciejewski, M., McBride, C., Neyrinck, M. C., Planelles, S., Potter, D., Quilis, V., Rasera, Y., Read, J. I., Ricker, P. M., Roy, F., Springel, V., Stadel, J., Stinson, G., Sutter, P. M., Turchaninov, V., Tweed, D., Yepes, G., and Zemp, M. Haloes gone MAD: The Halo-Finder Comparison Project. *Monthly Notices of the Royal Astronomical Society*, 415:2293–2318, August 2011. ISSN 0035-8711. doi: 10.1111/j.1365-2966.2011.18858.x.

Kobayashi, Y., Nishimichi, T., Takada, M., and Miyatake, H. Full-shape cosmology analysis of the SDSS-III BOSS galaxy power spectrum using an emulator-based halo model: A 5% determination of σ_8. , 105(8):083517, April 2022. doi: 10.1103/PhysRevD.105.083517.

Lemos, P., Coogan, A., Hezaveh, Y., and Perreault-Levasseur, L. Sampling-based accuracy testing of posterior estimators for general inference. *arXiv preprint arXiv:2302.03026*, 2023a.

Lemos, P., Cranmer, M., Abidi, M., Hahn, C., Eickenberg, M., Massara, E., Yallup, D., and Ho, S. Robust simulation-based inference in cosmology with bayesian neural networks. *Machine Learning: Science and Technology*, 4(1):01LT01, 2023b.

Li, Y., Lu, L., Modi, C., Jamieson, D., Zhang, Y., Feng, Y., Zhou, W., Pok Kwan, N., Lanusse, F., and Greengard, L. pmwd: A Differentiable Cosmological Particle-Mesh N-body Library. *arXiv e-prints*, art. arXiv:2211.09958, November 2022. doi: 10.48550/arXiv.2211.09958.

Maddox, W. J., Izmailov, P., Garipov, T., Vetrov, D. P., and Wilson, A. G. A simple baseline for bayesian uncertainty in deep learning. *Advances in neural information processing systems*, 32, 2019.

Madhavacheril, M. S., Qu, F. J., Sherwin, B. D., MacCrann, N., Li, Y., Abril-Cabezas, I., Ade, P. A. R., Aiola, S., Alford, T., Amiri, M., Amodeo, S., An, R., Atkins, Z., Austermann, J. E., Battaglia, N., Battistelli, E. S., Beall, J. A., Bean, R., Beringue, B., Bhandarkar, T., Biermann, E., Bolliet, B., Bond, J. R., Cai, H., Calabrese, E., Calafut, V., Capalbo, V., Carrero, F., Challinor, A., Chesmore, G. E., Cho, H.-m., Choi, S. K., Clark, S. E., Córdova Rosado, R., Cothard, N. F., Coughlin, K., Coulton, W., Crowley, K. T., Dalal, R., Darwish, O., Devlin, M. J., Dicker, S., Doze, P., Duell, C. J., Duff, S. M., Duivenvoorden, A. J., Dunkley, J., Dünner, R., Fanfani, V., Fankhanel, M., Farren, G., Ferraro, S., Freundt, R., Fuzia, B., Gallardo, P. A., Garrido, X., Givans, J., Gluscevic, V., Golec, J. E., Guan, Y., Hall, K. R., Halpern, M., Han, D., Harrison, I., Hasselfield, M., Healy, E., Henderson, S., Hensley, B., Hervías-Caimapo, C., Hill, J. C., Hilton, G. C., Hilton, M., Hincks, A. D., Hložek, R., Ho, S.-P. P., Huber, Z. B., Hubmayr, J., Huffenberger, K. M., Hughes, J. P., Irwin, K., Isopi, G., Jense, H. T., Keller, B., Kim, J., Knowles, K., Koopman, B. J., Kosowsky, A., Kramer, D., Kusiak, A., La Posta, A., Lague, A., Lakey, V., Lee, E., Li, Z., Limon, M., Lokken, M., Louis, T., Lungu, M., MacInnis, A., Maldonado, D., Maldonado, F., Mallaby-Kay, M., Marques, G. A., McMahon, J., Mehta, Y., Menanteau, F., Moodley, K., Morris, T. W., Mroczkowski, T., Naess, S., Namikawa, T., Nati, F., Newburgh, L., Nicola, A., Niemack, M. D., Nolta, M. R., Orlowski-Scherer, J., Page, L. A., Pandey, S., Partridge, B., Prince, H., Puddu, R., Radiconi, F., Robertson, N., Rojas, F., Sakuma, T., Salatino, M., Schaan, E., Schmitt, B. L., Sehgal, N., Shaikh, S., Sierra, C., Sievers, J., Sifón, C., Simon, S., Sonka, R., Spergel, D. N., Staggs, S. T., Storer, E., Switzer, E. R., Tampier, N., Thornton, R., Trac, H., Treu, J., Tucker, C., Ulluom, J., Vale, L. R., Van Engelen, A., Van Lanen, J., van Marrewijk, J., Vargas, C., Vavagiakis, E. M., Wagoner, K., Wang, Y., Wenzl, L., Wollack, E. J., Xu, Z., Zago, F., and Zhang, K. The Atacama Cosmology Telescope: DR6 Gravitational Lensing Map and Cosmological Parameters. *arXiv e-prints*, art. arXiv:2304.05203, April 2023.

Mallat, S. Understanding deep convolutional networks. *Philosophical Transactions of the Royal Society of London Series A*, 374(2065):20150203, April 2016. doi: 10.1098/rsta.2015.0203.

Massara, E., Villaescusa-Navarro, F., Ho, S., Dalal, N., and Spergel, D. N. Using the Marked Power Spectrum to Detect the Signature of Neutrinos in Large-Scale Structure. *arXiv:2001.11024 [astro-ph]*, January 2020.

Massara, E., Villaescusa-Navarro, F., Hahn, C., Abidi, M. M., Eickenberg, M., Ho, S., Lemos, P., Dizgah, A. M., and Blancard, B. R.-S. Cosmological Information in the Marked Power Spectrum of the Galaxy Field, June 2022.

Modi, C., Lanusse, F., and Seljak, U. FlowPM: Distributed TensorFlow implementation of the FastPM cosmological N-body solver. *Astronomy and Computing, Volume 37, article id. 100505.*, 37:100505, October 2021. ISSN 2213-1337. doi: 10.1016/j.ascom.2021.100505.

Navarro, J. F., Frenk, C. S., and White, S. D. M. A Universal Density Profile from Hierarchical Clustering. *The Astrophysical Journal*, 490(2):493, December 1997. doi: 10.1086/304888.

Page, L., Barnes, C., Hinshaw, G., Spergel, D., Weiland, J., Wollack, E., Bennett, C., Halpern, M., Jarosik, N., Kogut, A., et al. First-year wilkinson microwave anisotropy probe (wmap)* observations: Beam profiles and window functions. *The Astrophysical Journal Supplement Series*, 148(1):39, 2003.

Papamakarios, G., Pavlakou, T., and Murray, I. Masked Autoregressive Flow for Density Estimation. *arXiv e-prints*, 1705:arXiv:1705.07057, May 2017.

Perlmutter, S., Aldering, G., Goldhaber, G., Knop, R., Nugent, P., Castro, P. G., Deustua, S., Fabbro, S., Goobar, A., Groom, D. E., et al. Measurements of ω and λ from 42 high-redshift supernovae. *The Astrophysical Journal*, 517(2):565, 1999.

Riess, A. G., Filippenko, A. V., Challis, P., Clocchiatti, A., Diercks, A., Garnavich, P. M., Gilliland, R. L., Hogan, C. J., Jha, S., Kirshner, R. P., et al. Observational evidence from supernovae for an accelerating universe and a cosmological constant. *The astronomical journal*, 116 (3):1009, 1998.

Ross, A. J., Percival, W. J., Sánchez, A. G., Samushia, L., Ho, S., Kazin, E., Manera, M., Reid, B., White, M., Tojeiro, R., McBride, C. K., Xu, X., Wake, D. A., Strauss, M. A., Montesano, F., Swanson, M. E. C., Bailey, S., Bolton, A. S., Dorta, A. M., Eisenstein, D. J., Guo, H., Hamilton, J.-C., Nichol, R. C., Padmanabhan, N., Prada, F., Schlegel, D. J., Magaña, M. V., Zehavi, I., Blanton, M., Bizyaev, D., Brewington, H., Cuesta, A. J., Malanushenko, E., Malanushenko, V., Oravetz, D., Parejko, J., Pan, K., Schneider, D. P., Shelden, A., Simmons, A., Snedden, S., and Zhao, G.-b. The clustering of galaxies in the SDSS-III Baryon Oscillation Spectroscopic Survey: Analysis of potential systematics. *Monthly Notices of the Royal Astronomical Society*, 424:564–590, July 2012. ISSN 0035-8711. doi: 10.1111/j.1365-2966.2012.21235.x.

Ross, A. J., Beutler, F., Chuang, C.-H., Pellejero-Ibanez, M., Seo, H.-J., Vargas-Magaña, M., Cuesta, A. J., Percival, W. J., Burden, A., Sánchez, A. G., Grieb, J. N., Reid, B., Brownstein, J. R., Dawson, K. S., Eisenstein, D. J., Ho, S., Kitaura, F.-S., Nichol, R. C., Olmstead, M. D., Prada, F., Rodríguez-Torres, S. A., Saito, S., Salazar-Albornoz, S., Schneider, D. P., Thomas, D., Tinker, J., Tojeiro, R., Wang, Y., White, M., and Zhao, G.-b. The clustering of galaxies in the completed SDSS-III Baryon Oscillation Spectroscopic Survey: Observational systematics and baryon acoustic oscillations in the correlation function. *Monthly Notices of the Royal Astronomical Society*, 464: 1168–1191, January 2017. ISSN 0035-8711. doi: 10.1093/mnras/stw2372.

Schaurecker, D., Li, Y., Tinker, J., Ho, S., and Refregier, A. Super-resolving Dark Matter Halos using Generative Deep Learning, November 2021.

Schöneberg, N., Lesgourgues, J., and Hooper, D. C. The BAO+BBN take on the Hubble tension. , 2019(10):029, October 2019. doi: 10.1088/1475-7516/2019/10/029.

Scoccimarro, R. Fast Estimators for Redshift-Space Clustering. *Physical Review D*, 92(8), October 2015. ISSN 1550-7998, 1550-2368. doi: 10.1103/PhysRevD.92.083532.

Shah, P., Lemos, P., and Lahav, O. A buyer's guide to the Hubble constant. *Astron. Astrophys. Rev.*, 29(1):9, 2021. doi: 10.1007/s00159-021-00137-4.

Tabak, E. G. and Turner, C. V. A Family of Nonparametric Density Estimation Algorithms. *Communications on Pure and Applied Mathematics*, 66(2):145–164, 2013. ISSN 1097-0312. doi: 10.1002/cpa.21423.

Tabak, E. G. and Vanden-Eijnden, E. Density estimation by dual ascent of the log-likelihood. *Communications in Mathematical Sciences*, 8(1):217–233, March 2010. ISSN 1945-0796. doi: 10.4310/CMS.2010.v8.n1.a11.

Talts, S., Betancourt, M., Simpson, D., Vehtari, A., and Gelman, A. Validating Bayesian Inference Algorithms with Simulation-Based Calibration. *arXiv:1804.06788 [stat]*, October 2020.

Tejero-Cantero, A., Boelts, J., Deistler, M., Lueckmann, J.-M., Durkan, C., Gonçalves, P. J., Greenberg, D. S., and Macke, J. H. Sbi: A toolkit for simulation-based inference. *Journal of Open Source Software*, 5(52):2505, August 2020. ISSN 2475-9066. doi: 10.21105/joss.02505.

Villaescusa-Navarro, F., Hahn, C., Massara, E., Banerjee, A., Delgado, A. M., Ramanah, D. K., Charnock, T., Giusarma, E., Li, Y., Allys, E., Brochard, A., Uhlemann, C., Chiang, C.-T., He, S., Pisani, A., Obuljen, A., Feng, Y., Castorina, E., Contardo, G., Kreisch, C. D., Nicola, A., Alsing, J., Scoccimarro, R., Verde, L., Viel, M., Ho, S., Mallat, S., Wandelt, B., and Spergel, D. N. The Quijote Simulations. *The Astrophysical Journal Supplement Series*, 250:2, September 2020. doi: 10.3847/1538-4365/ab9d82.

Wang, Y., Zhao, G.-B., Koyama, K., Percival, W. J., Takahashi, R., Hikage, C., Gil-Marín, H., Hahn, C., Zhao, R., Zhang, W., Mu, X., Yu, Y., Zhu, H.-M., and Ge, F. Extracting high-order cosmological information in galaxy surveys with power spectra, February 2022.

Wilson, A. G. and Izmailov, P. Bayesian deep learning and a probabilistic perspective of generalization. *Advances in neural information processing systems*, 33:4697–4708, 2020.

Zheng, Z., Coil, A. L., and Zehavi, I. Galaxy Evolution from Halo Occupation Distribution Modeling of DEEP2 and SDSS Galaxy Clustering. *The Astrophysical Journal*, 667:760–779, October 2007. ISSN 0004-637X. doi: 10.1086/521074.

A. Details on the Forward Models

The SIMBIG forward model constructs simulated galaxy catalogs from QUIJOTE N-body simulations (Villaescusa-Navarro et al., 2020) run at different cosmologies in a Latin-hypercube configuration. Each simulation has a volume of $1(h^{-1}\mathrm{Gpc})^3$ and is constructed using 1024^3 cold dark matter (CDM) particles initialized at $z = 127$ using 2LPT and gravitationally evolved until $z = 0.5$. From the N-body simulations, halos are identified using the phase space information of dark matter particles with the ROCKSTAR halo finder (Behroozi et al., 2013). Afterwards, the halos are populated using the halo occupation distribution (HOD; Berlind & Weinberg, 2002; Zheng et al., 2007) framework, which provides a flexible statistical prescription for determining the number of galaxies as well as their positions and velocities within halos.

SIMBIG use a state-of-the art 9 parameter HOD model that supplements the standard (Zheng et al., 2007) model with assembly, concentration, and velocity biases. The number of central and satellite galaxies in a halo is determined by its mass and HOD parameters. Central galaxies are placed at the center of the halos while satellite galaxies are placed according to a (Navarro et al., 1997) profile. On top of this, the SIMBIG HOD model includes assembly bias using the (Hearin et al., 2016) decorated HOD prescription so that galaxy occupation depends on halo concentration, a proxy for its assembly history, in addition to its mass. The model also includes concentration bias, which allow the concentration of satellites galaxies to deviate from the NFW profile. Lastly, it also includes central and satellite velocity biases that allow the velocity of centrals and satellites to be rescaled with respect to the host halo.

From the HOD galaxy catalog, SIMBIG then adds full BOSS survey realism by applying the survey geometry and observational systematics. The forward modeled catalogs have the same redshift range and angular footprint of our observed sample, including masking for bright stars, centerpost, bad field, and collision priority. Furthermore, SIMBIG also includes fiber collisions, which systematically removes galaxies in galaxy pairs within an angular scale of $62''$.

The SIMBIG forward model is based on high resolution N-body simulations that accurately model the clustering of matter down to non-linear scales beyond $k = 0.5\,h/\mathrm{Mpc}$ (Villaescusa-Navarro et al., 2020). It also uses halos identified using ROCKSTAR which has been shown to accurately determine the location of halos and resolve their substructure (Knebe et al., 2011). Furthermore, galaxies are populated using a highly flexible HOD model. Lastly, observational systematics are included in the forward model. With these features, the SIMBIG forward model can generate mock galaxy catalogs that are statistically indistinguishable from the observations. For further details on the forward model, we refer readers to (Hahn et al., 2022) and (Hahn et al., 2023).

B. Details on Simulation-Based Inference

From the forward modeled galaxy catalogs, we use the SIMBIG SBI framework to infer posterior distributions of cosmological parameters for given a summary statistic of the observations: $p(\boldsymbol{\theta}\,|\,\boldsymbol{x})$. The SBI framework enables cosmological inference with a limited number of simulated forward models. This enables us to extract cosmological information on small, non-linear, scales and using higher-order statistics, beyond standard cosmological analyses.

The SBI in SIMBIG is based on neural density estimation and uses "normalizing flow" models (Tabak & Vanden-Eijnden, 2010; Tabak & Turner, 2013). Normalizing flows use neural networks to learn an extremely flexible and bijective transformation, f, that maps a complex target distribution to a simple base distribution, $\pi(\boldsymbol{z})$, that is fast to evaluate. f is defined to be invertible and have a tractable Jacobian so that the target distribution can be evaluated from $\pi(\boldsymbol{z})$ by change of variables. Since $\pi(\boldsymbol{z})$ is easy to evaluate, this enables us to also easily evaluate the target distribution. In our case, the target distribution is the posterior and the base distribution is a multivariate Gaussian. Among various normalizing flow architectures, SIMBIG uses Masked Autoregressive Flow (MAF; Papamakarios et al., 2017) models.[2]

Our goal is to train a normalizing flow that best approximates the posterior, $p(\boldsymbol{\theta}\,|\,\boldsymbol{x}) \approx q_{\boldsymbol{\phi}}(\boldsymbol{\theta}\,|\,\boldsymbol{x})$, by minimizing the KL divergence between $p(\boldsymbol{\theta}, \boldsymbol{x}) = p(\boldsymbol{\theta}\,|\,\boldsymbol{x})p(\boldsymbol{x})$ and $q_{\boldsymbol{\phi}}(\boldsymbol{\theta}\,|\,\boldsymbol{x})p(\boldsymbol{x})$. In practice, we first split the forward modeled catalogs into a training and validation set with a 90/10 split. Then we maximize the total log-likelihood $\sum_i \log q_{\boldsymbol{\phi}}(\boldsymbol{\theta}_i\,|\,\boldsymbol{x}_i)$ over the training set, which is equivalent to the KL divergence, using the ADAM optimizer (Kingma & Ba, 2017) with a learning rate of 5×10^{-4}. To prevent overfitting, we evaluate the total log-likelihood on the validation data at every training epoch and stop the training when the validation log-likelihood fails to increase after 20 epochs.

We determine the architecture of our normalizing flow through experimentation. We train a large number of flows with architectures determined using the (**?**) hyperparameter optimization framework and select the five normalizing flows with

[2] We use the MAF implementation in `sbi` Python package[3] (Greenberg et al., 2019; Tejero-Cantero et al., 2020).

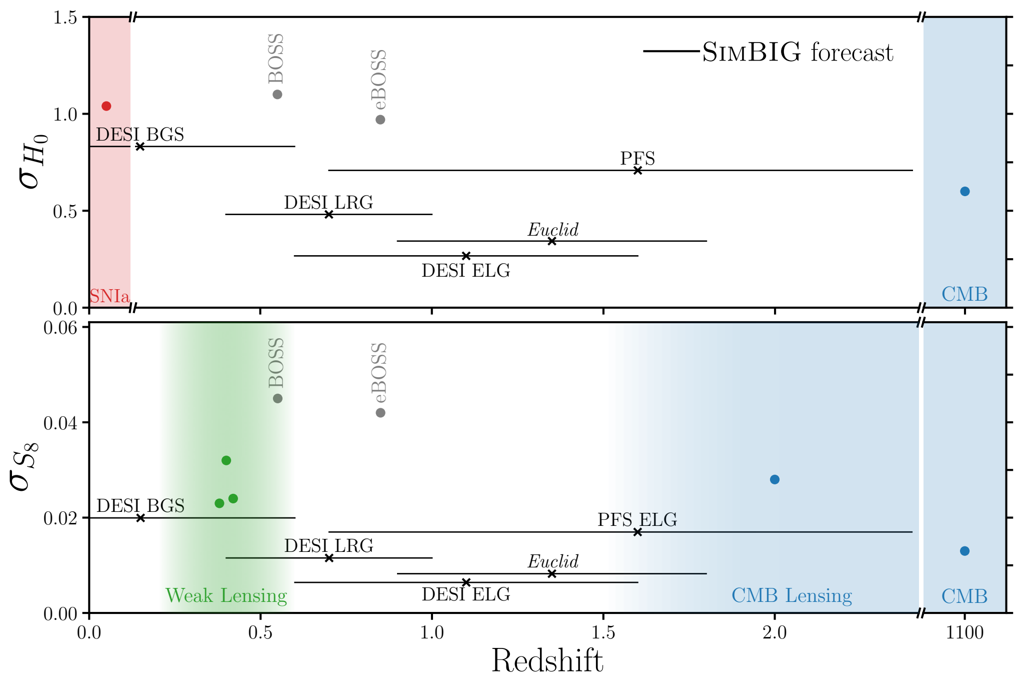

Figure 4. Expected 1σ precision level of H_0 (σ_{H_0}; top) and S_8 (σ_{S_8}; bottom) constraints from applying SIMBIG to upcoming galaxy surveys, DESI, PFS, *Euclid* (black). The width of σ_{H_0} and σ_{S_8} marks the redshift range of each sample. In the top panel, we include σ_{H_0} from the SH0ES SNIa (red), *Planck* CMB (blue), and P_ℓ analyses (gray), for comparison. In the bottom panel, we include σ_{S_8} from weak lensing (green), CMB and CMB lensing (blue), and P_ℓ analyses (gray), for comparison. Future SIMBIG analyses will have the precision and redshift range to provide key input into the H_0 and S_8 tensions and potentially reveal new physics beyond ΛCDM.

the lowest validation losses. Our final flow is an equally weighted ensemble of the flows: $q_{\boldsymbol{\phi}}(\boldsymbol{\theta}\,|\,\boldsymbol{x}) = \sum_{i=1}^{5} q_{\phi}^{i}(\boldsymbol{\theta}\,|\,\boldsymbol{x})/5$. We find that ensembling flows with different initializations and architectures improves the overall robustness of our normalizing flow.